Multi-month forecasts of marine heatwaves and ocean acidification extremes

Samuel C Mogen[1*], Nicole S Lovenduski[1], Stephen Yeager[2], Antonietta Capotondi [3,4], Michael G. Jacox[4,5], Steven J. Bograd[5], Emanuele Di Lorenzo[6], Elliott L. Hazen[5], Mercedes Pozo Buil[5,7], Who Kim[2], Nan Rosenbloom[2]

[1] Department of Atmospheric and Oceanic Sciences and Institute of Arctic and Alpine Research, University of Colorado, Boulder, CO, USA
[2] NSF National Center for Atmospheric Research, Climate and Global Dynamics Lab, Boulder, CO, USA
[3] Cooperative Institute for Research in Environmental Sciences, University of Colorado Boulder, Boulder, CO, USA
[4] National Oceanic and Atmospheric Administration Physical Sciences Laboratory, Boulder, CO, USA
[5] National Oceanic and Atmospheric Administration Southwest Fisheries Science Center, Monterey, CA, USA
[6] Department of Earth, Environmental, and Planetary Sciences Brown University, Providence, RI, USA
[7] Institute of Marine Sciences, University of California Santa Cruz, Monterey, CA, USA
[*] Corresponding author: samuel.mogen@colorado.edu

Abstract

Marine heatwaves and ocean acidification extreme events are periods during which temperature and acidification reach statistically extreme levels (90^{th} percentile), relative to normal variability, potentially endangering ecosystems. As the threats from marine heatwaves and ocean acidification extreme events grow with climate change, there is need for skillful predictions of events months-to-years in advance. Previous work has demonstrated that climate models can predict marine heatwaves up to 12 months in advance in key regions, but forecasting of ocean acidification extreme events has been difficult due to the sparse observational record. Here we use the Community Earth System Model Seasonal-to-Multiyear Large Ensemble to make predictions of marine heatwaves and two forms of ocean acidification extreme events, as defined by anomalies in hydrogen ion concentration and aragonite saturation state. We show that the ensemble skillfully predicts marine heatwaves and ocean acidification extreme events as defined by aragonite saturation state up to 1 year in advance. Predictive skill for ocean acidification extremes as defined by hydrogen ion concentration is lower, likely reflecting mismatch between model and observed state. Skill is highest in the eastern Pacific, reflecting the predictable contribution of El Niño-Southern Oscillation to regional variability. A forecast generated in late 2023 during the 2023-24 El Niño event finds high likelihood for widespread marine heatwaves and ocean acidification extreme events in 2024.

Alongside long-term alterations to the marine system associated with anthropogenic climate change [1–4], there is increasing concern for short-term extreme events that can have dramatic impacts on marine ecosystems [5–7]. Accurate forecasts of extreme events have the potential to alter management practices in advance to plan for, if not mitigate, impacts on marine ecosystems [8]. Marine heatwaves (MHWs), extremes in ocean temperature, are relatively well-studied and driven by a variety of atmospheric and oceanic dynamical processes [9–14]. Marine heatwaves can have profound impacts on marine organisms and ecosystems. They have been shown to alter primary productivity [15], stress keystone species [16], and induce dramatic species redistribution [17]. They can also impact regional biodiversity [18] and biogeochemistry [5] in the surface and subsurface ocean [19].

In contrast, ocean acidification extremes (OAX) are relatively under-studied, due in part to a historically limited observational record, although recent literature discusses the development, location, and impacts of OAX [20–26]. Previous work has focused on two forms of OAX: high hydrogen ion concentration ($[H^+]$) and low saturation state of seawater in relation to the carbonate mineral aragonite (Ω_a). Ω_a is the degree

of saturation of seawater with respect to the mineral aragonite [27]; high values of Ω_a support aragonite shell maintenance, while low values are associated with aragonite shell dissolution. Calcifying organisms are negatively impacted during periods characterized by anomalously low Ω_a [28–30]. Both $[H^+]$ and Ω_a are important measures of acidification with differing impacts on, and responses from, marine organisms [23, 31, 32]. For example, pteropods, a type of aragonitic zooplankton, respond to variations in both Ω_a (impacting shell growth, dissolution, and survival [32–34]) and $[H^+]$ (impacting embryonic development [35]). While extremes in $[H^+]$ and Ω_a may co-occur [24], they are commonly driven by different physical processes [23]. The drivers of extremes in $[H^+]$ vary regionally. Subtropical $[H^+]$ extremes are generally driven by increased temperatures while advection of carbon-rich water is the primary control in the tropics and mid-to-high latitudes (where vertical mixing also plays a role). Extremes in Ω_a are globally driven by enhanced vertical mixing of carbon-rich subsurface water [23]. As such, while the occurrence of MHW may be regionally tied to OAX (e.g. co-occurring $[H^+]$ extremes and MHW in the subtropics [23]), OAX are also driven by enhanced vertical mixing and advection (which are often suppressed during MHW).

Initialized Earth system model (ESM) forecasts simulate the evolution of the coupled carbon-climate system from a baseline state of historical model reconstruction, and have demonstrated skillful seasonal-to-interannual forecasts of marine stressors, including temperature [36, 37] and ocean acidification [37, 38]. Jacox et al. 2022 [8] skillfully forecast surface marine heatwaves up to one year in advance using the physics-only North American Multi-model Ensemble (NMME), a collection of global climate model forecasts. They find that MHW forecast skill is dependent on El Nino-Southern Oscillation (ENSO) state. Similarly, McAdam et al. 2023 [39] used the CMCC Seasonal Prediction System version 3.5 (CMCC-SPS3.5) and found high potential for predicting subsurface heatwaves. No previous work has examined the forecast skill and predictability of OAX.

Here, we use the Community Earth System Model (CESM) Seasonal to Multiyear Large Ensemble (SMYLE) to forecast surface ocean MHW and OAX (both $[H^+]$ and Ω_a) events. CESM SMYLE generates forecasts of the short-term evolution of the Earth system, initialized from a reconstruction of the historical ocean (SMYLE FOSI) [40]. CESM SMYLE has previously demonstrated high forecast skill for biogeochemical (dissolved oxygen, dissolved inorganic carbon) and physical tracers (temperature) in both the surface and subsurface ocean up to a year following initialization [37, 40]. CESM SMYLE has also demonstrated high forecast skill for ENSO anomalies, performing similarly to other seasonal forecast systems [40]. Here, model forecasts are validated with observations over the historical period for extreme events in the surface ocean at the 90^{th} percentile threshold. We find regions of notably high forecast skill over the historical record, including in the eastern tropical and northeast Pacific. We use forecasts generated in late 2023 to assess the likelihood of global MHW and OAX in the coming year, finding high likelihood for widespread marine extremes throughout 2024.

0.1 Skillful forecasts of MHW and OAX

CESM SMYLE skillfully forecasts surface MHW and OAX (Ω_a) up to a year in advance regionally, while OAX ($[H^+]$) has generally lower forecast skill (Figure 1). Using the Symmetric Extremal Dependence Index (SEDI; Methods), we find significant skill relative to 1,000 random forecasts at the 95% confidence interval 1.5 months after initialization for MHW and OAX (Ω_a) globally, with lower global skill in OAX ($[H^+]$) (Figure 1, row 1). Skill degrades with forecast lead-time, though MHW forecasts remain significantly skillful in the eastern tropical, northeastern, and southeastern Pacific up to 10.5 months after initialization (Figure 1). Similarly, OAX (Ω_a) skill remains significant in the central tropical, northeast, and south Pacific for up to 10.5 months; with skill noticeably higher in the northeast Pacific than for MHW forecasts. In contrast, OAX ($[H^+]$) skill is globally lower 1.5 months after initialization and further degrades with forecast lead-time, with limited significant forecast skill in the eastern tropical Pacific at all lead times (Figure 1; 3^{rd} column).

Two other metrics of model skill - forecast accuracy and Brier Skill Score - support results from SEDI (Figure S1, Methods), with the tropical Pacific exhibiting high skill for MHW and OAX (Ω_a), and generally lower skill for OAX ($[H^+]$). CESM SMYLE also successfully estimates the typical frequency and intensity for historical MHW and OAX, but consistently overestimates the duration of these extreme events at a given location (Figure S2).

MHW forecast skill is comparable to that reported by Jacox et al, 2022 [8], with similar regions (e.g. the eastern tropical Pacific) demonstrating significant and long-lasting skill for MHW. OAX (Ω_a) skill mirrors that of MHW, while OAX ($[H^+]$) shows distinct patterns. Regions shown to be skillful in CESM SMYLE correspond to those that exhibit high correlation in the temporal variability and occurrence of extremes between SMYLE FOSI, the historical reconstruction used in initializing CESM SMYLE, and observations, including the tropical and northeast Pacific (Figure S3). MHW and OAX (Ω_a) forecasts are thus expected to demonstrate higher

skill because CESM2 can successfully recreate these events in the tropical and northeast Pacific in the FOSI state estimate.

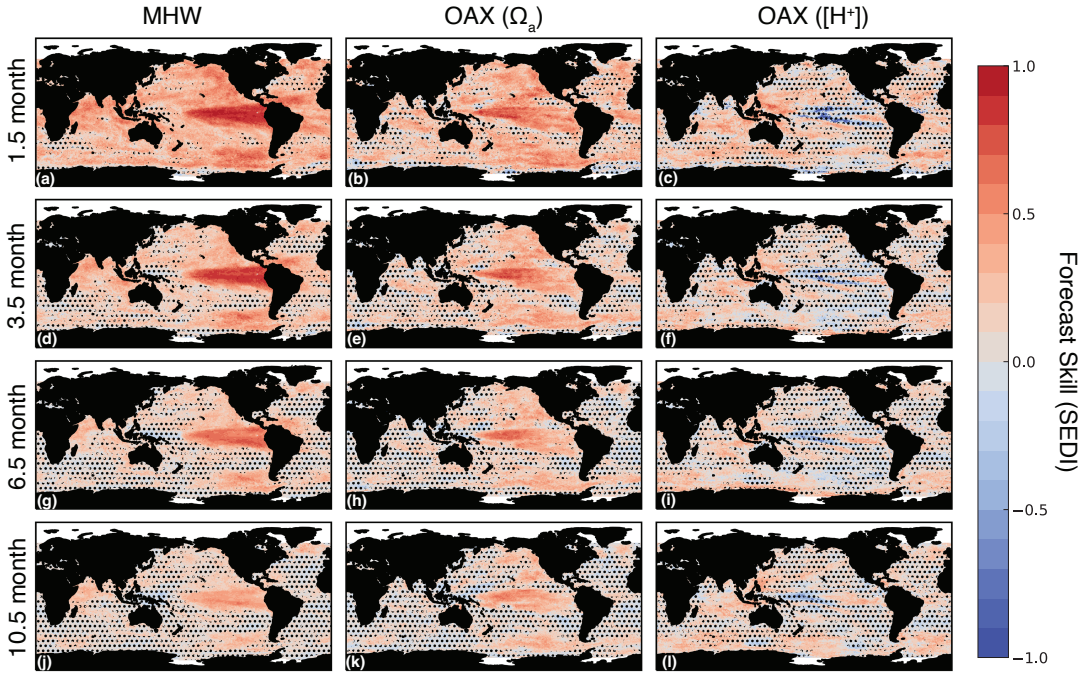

Figure 1: Forecast skill (SEDI) for MHW (column 1), ocean acidification extremes (Ω_a) (column 2), and ocean acidification extremes ($[H^+]$) (column 3) for 20 ensemble members from CESM SMYLE at 1.5 (a-c), 3.5 (d-f), 6.5 (g-i), and 10.5 month lead-time (j-l). Skill scores range from -1 to 1, with skill close to -1 being unskillful, skill of 0 being no better than random forecasts, and skill of 1 being perfect skill. Dots indicate where skill is not significantly better than random forecasts at the 95% confidence interval.

0.2 Drivers of skillful forecasts

What is driving high and long-lasting skill in MHW and OAX (Ω_a) and low skill in OAX ($[H^+]$)? As noted in prior work, ENSO imprints on the seasonal-to-multiyear forecast skill for physical and biogeochemical variability, and has been linked to MHW in regions including the tropical and northeast Pacific [8, 37, 41], although the ENSO influence in the Northeast Pacific may be mediated by North Pacific decadal variability [42–44]. Further, the highest correlations in the historical occurrence of variability and extreme events between the SMYLE FOSI model reconstruction and observations (Figure S3), as well as the highest extreme event forecast skill (Figure 1), occur in regions associated with ENSO-based variability in the tropical Pacific. ENSO is thus likely an important driver of forecast skill in the tropical and northeast Pacific.

We examine the dominant modes of variability in our variables of interest in the tropical Pacific (region bounded by latitude 30^{o}S-30^{o}N and longitude 140^{o}E-280^{o}E) to illustrate the relationship between physics and biogeochemistry, and their linkages to ENSO, using EOF analysis of SMYLE FOSI (Figure 2; Methods). The dominant modes of variability in tropical Pacific SST and Ω_a anomalies are characterized by a similar spatial pattern reminiscent of ENSO (Figure 2a,d). Indeed, the first principal components of SST and Ω_a anomalies are highly correlated with the Nino3.4 index ($r_{SST} = 0.84$, $p < 0.05$; $r_{\Omega_a} = 0.75$, $p < 0.05$). Meanwhile, the dominant mode of variability in tropical Pacific [H$^+$] anomalies exhibits a different spatial pattern, and its first principal component has a much lower correlation with the Nino3.4 index ($r_{[H^+]} = 0.07$, $p > 0.05$) (Figure 2b,f), although we note a higher correlation when lagged by 9-months ($r_{[H^+],\,9\,month\,lag} = 0.65$, $p > 0.05$).

Marine heatwaves induce direct changes in $[H^+]$ by altering the carbonate chemistry equilibrium constants [23, 45, 46]. When marine heatwaves are driven by ocean circulation processes (e.g., stratification of the upper ocean, reduced upwelling), the circulation of inorganic carbon is also affected which can have an indirect influence on both $[H^+]$ and Ω_a [23, 46]. We demonstrate that circulation-driven $[H^+]$ variability

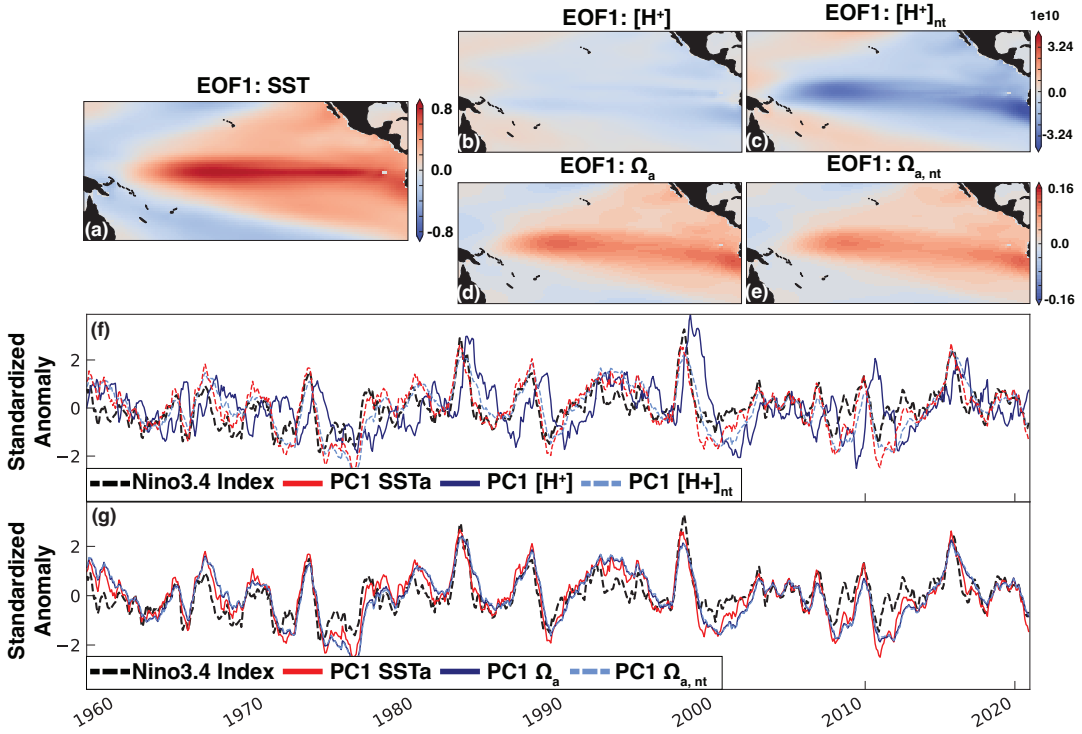

Figure 2: Dominant modes of tropical Pacific variability in SMYLE FOSI from principal component analysis. The first Empirical Orthogonal Function (EOF) regressed onto anomalies is displayed for (a) SST , (b) Ω_a, (c) $\Omega_{a,nt}$, (d) $[H^+]$, and (e) $[H^+]_{nt}$ variability in the tropical Pacific region. (f) The first Principal Component of tropical Pacific (red) SST, (blue) $[H^+]$, and (blue dashed) $[H^+]_{nt}$ variability, and (black dashed) the Niño3.4 index. (g) as in (f) but for (blue) Ω_a and (blue dashed) $\Omega_{a,nt}$.

is closely tied to Nino3.4 by performing EOF analysis on tropical Pacific nonthermal $[H^+]$ ($[H^+]_{nt}$), where the direct effects of temperature on the equilibrium constants have been removed from $[H^+]$. The leading EOF of tropical Pacific $[H^+]_{nt}$ variability has a spatial pattern similar to that of Ω_a (Figure 2c,d), with the first principal component more highly correlated with Nino3.4 ($r_{[H^+]_{nt}} = 0.71$, $p < 0.05$) than $[H^+]$. In contrast, Ω_a variability is unaffected by temperature variability, as the first principal component of both Ω_a and $\Omega_{a,nt}$ are highly correlated with the Nino3.4 index ($r_{\Omega_{a,nt}} = 0.73, p < 0.05$, $r_{\Omega_a} = 0.75$, $p < 0.05$). While we do not attempt to forecast $[H^+]_{nt}$ using CESM SMYLE (a forecast of $[H^+]_{nt}$ would offer little practical information), we would nevertheless expect higher SEDI skill score values. As the primary modes of tropical Pacific variability of SST, Ω_a, $\Omega_{a,nt}$ and $[H^+]_{nt}$ exhibit strong spatial and temporal correlations with ENSO, we expect forecasts made during ENSO events (both El Niño and La Niña) to be more skillful than those made during neutral conditions. We thus systematically determine the differences in skill when the model is initialized during (positive or negative) ENSO or neutral ENSO conditions.

In many regions, there is a gain in skill when an extreme event forecast is generated during ENSO (El Niño or La Niña) conditions, demonstrating the role of ENSO in engendering skillful forecasts of MHW and OAX as in Jacox et al. 2022 [8] (Figure 3, Methods). MHWs show a gain in skill during ENSO conditions for the first year of model integration, most notably in the tropical Pacific. Gain in MHW forecast skill increases for up 10.5 lead-months after initialization, implying that forecast initialization during an ENSO event drives long-lasting gains in skill. OAX (Ω_a) also demonstrates some regional gains in skill when initialized during an ENSO event, particularly in the eastern tropical Pacific, California Current, and Gulf of Alaska regions. Similarly, OAX ($[H^+]$) demonstrate regional gains in skill during ENSO events. Surprisingly, the gain in skill for OAX ($[H^+]$) manifests more broadly than that of OAX (Ω_a) despite the latter being consistently more skillful at all lead times (per Figure 1) and the weaker relationship between modeled $[H^+]$ variability and ENSO (Figure 2). Although OAX ($[H^+]$) does exhibit a stronger gain in skill, absolute skill scores are still relatively low compared to OAX (Ω_a) (as reflected in the magnitude of skill in Figure 1).

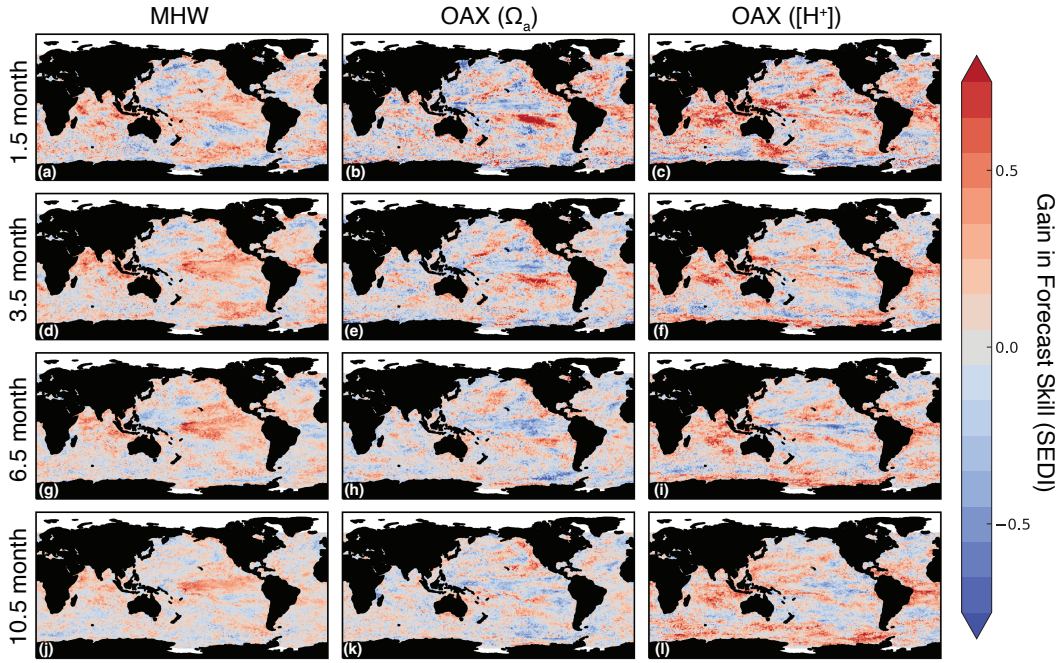

Figure 3: Gain in SEDI forecast skill from forecasts initialized during ENSO events (El Niño or La Niña) relative to forecasts initialized during neutral ENSO conditions. Gain in skill is displayed for (column 1) marine heatwaves, (column 2) ocean acidification extremes (Ω_a), and (column 3) ocean acidification extremes ($[H^+]$) at (a-c) 1.5 months lead-time, (d-f) 3.5 months lead-time, (g-i) 6.5 months lead-time, and (j-l) 10.5 months lead-time. Positive values indicate a gain in forecast skill during ENSO conditions, while negative values indicate gain in forecast skill during neutral conditions.

Our analysis shows that the two indicators of OAX are not forecast equally well, and they do not respond identically to ENSO variability, with OAX defined by extremes in Ω_a exhibiting higher forecast skill than those defined using $[H^+]$. Both indicators of OAX are important stressors for marine ecosystems - why can we only predict one? OAX ($[H^+]$) forecast skill is low due to the model's inability to capture observed $[H^+]$ variability. Figure S4 demonstrate high model predictability, illustrating that forecasts of $[H^+]$ extremes have the potential to be skillful across the global ocean (predictability is determined by verifying CESM SMYLE forecasts against SMYLE FOSI). However this potential predictability is not realized as forecast skill. As such, improvements in the model representation of $[H^+]$ variability to better match observed variability could increase the forecast skill of OAX ($[H^+]$). High skill for OAX (Ω_a), in contrast, corresponds to low model bias in Ω_a variability (Figures S3). Changes in Ω_a during extreme events are primarily driven by variations in $[CO_3]^{2-}$, which in turn derive primarily from variability in DIC (Figure S5). During OAX (Ω_a), the DIC circulation tendency affects change in surface ocean DIC, with air-sea CO2 flux and biology playing less important roles in the anomalous DIC budget. These results inform future studies on the utility of OAX forecasts for marine managers.

0.3 Outlook for extreme events in 2024

Forecasts generated in November of 2023 predict widespread MHW and OAX (Ω_a) events in 2024 (Figure 4). As these forecasts were generated during El Niño event, we expect forecasts of MHW and OAX (Ω_a) to have high skill in regions with ENSO-related predictability (as in Figure 1). The 2023-2024 ENSO event represents an excellent test-bed and application for an initialized ESM to forecast marine extreme events, as we can expect a forecast generated in late 2023 to be skillful in some regions up to a year in advance. The 2023-24 El Niño in CESM SMYLE is forecast to peak in January, 2024 before declining by June 2024 (Figure 4, panel a). This forecast is consistent with a suite of available dynamical ENSO forecasts generated in November, 2023, indicating a peak in El Niño centered in January, 2024 with decline in conditions by June, 2024, and is further consistent with the evolution of the Nino3.4 index derived from observations through March, 2024 (https://stateoftheocean.osmc.noaa.gov/sur/pac/nino34.php) [47].

CESM SMYLE forecasts indicate that MHWs are highly likely in the eastern Pacific in early 2024, before becoming globally widespread (Figure 4, column 2). In these forecasts, we find a strong signal of ENSO-driven MHWs (present at the month initialization) in the eastern tropical Pacific that spreads throughout the tropical Pacific through June 2024. The ENSO-associated teleconnections lead to strong and widespread MHWs in the Northeast Pacific by June 2024. OAX (Ω_a) are projected to be widespread by the middle of 2024 (Figure 4, column 3). The initial stages of this El Niño event are associated with widespread OAX events (e.g. in the Indian, and subtropical Pacific), though not in the eastern Tropical Pacific (likely connected to surface warming in the eastern tropical Pacific suppressing low Ω_a conditions [48]). By December 2024, we forecast extreme conditions in Ω_a in the Northeast Pacific and equatorial Atlantic. While we limit our forecast analysis to the 13 months following initialization in November, 2023, a subsequent La Niña event would likely be associated with strong OAX events in the eastern Pacific (as in the historical record in Figure S6, which shows an example forecast generated during the 1999-2000 La Niña event with widespread OAX event in the eastern Pacific).

Managing marine systems in the coming decades will require improved and expanded forecasts that include marine stressors beyond temperature [49]. The forecasts displayed in Figure 4 should encourage plans to expand existing operational forecasting systems (e.g., psl.noaa.gov/marine-heatwaves/#forecasts, and https://www.mercator-ocean.eu/en/category/mhw-bulletin/) to represent marine biogeochemistry, allowing for outlooks on extremes in key ecosystem stressors. Accurate forecasts of marine dynamics and extremes can better inform contemporary practices of marine managers, especially in a changing climate [8, 50, 51]. While our study does not make concrete policy recommendations, we hope that this work encourages the inclusion of biogeochemical and carbon cycle models in operational forecasts and seasonal outlooks that currently only include physical tracers. While OAX are less well-studied than MHW, they are demonstrably predictable and have potentially dramatic ramifications for ecosystems. Future studies should focus on forecasting concurrent extremes, especially those that are dynamically favored to co-occur (e.g. MHW and OAX $[H^+]$), and examine underlying definitions of extreme events (e.g. potentially using an absolute rather than statistical definition of an extreme). As operational forecasts of MHW become more mainstream (as at NOAA Physical Sciences Lab and Mercator Ocean International), the inclusion of biogeochemical extremes would help better inform the health of marine ecosystems.

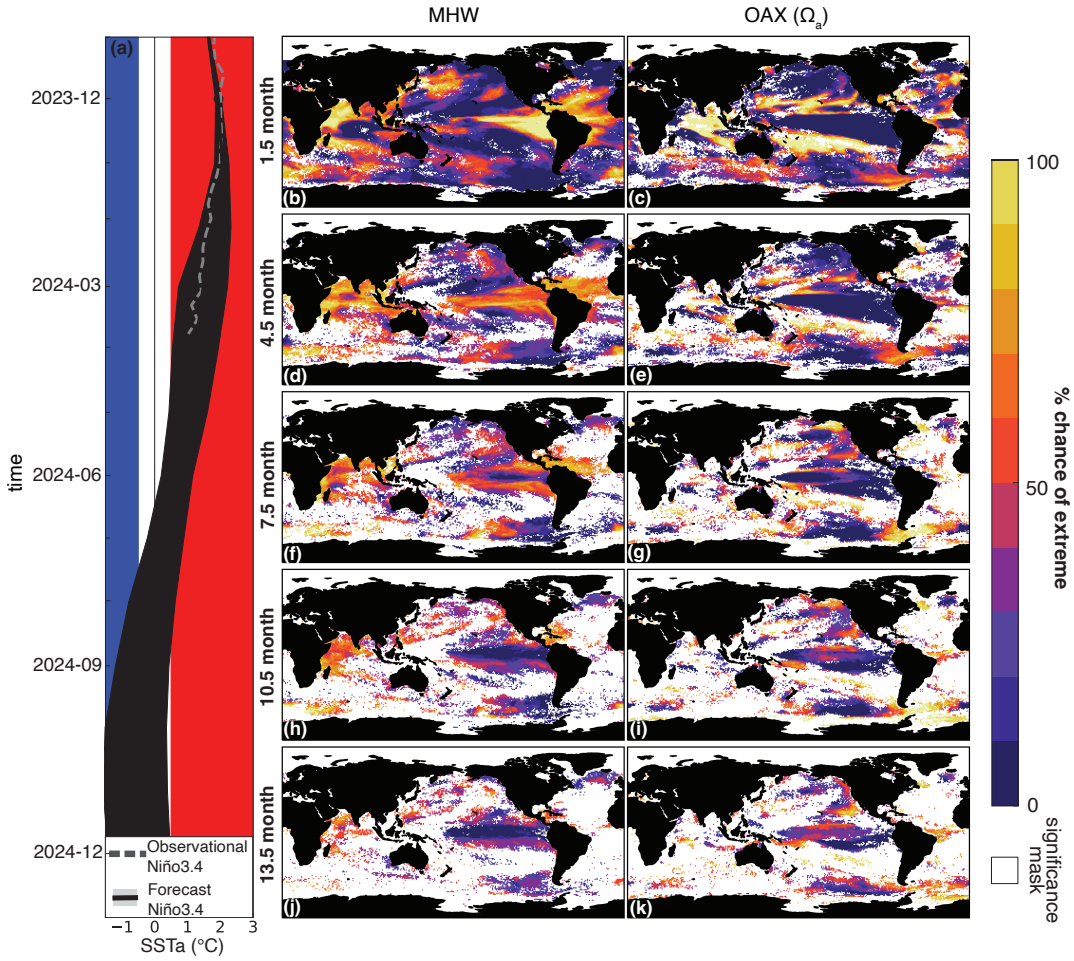

Figure 4: CESM SMYLE forecasts of Niño3.4, MHW, and OAX initialized in November 2023 from 60^{o}S to 60^{o}N. (a) Niño3.4 sea surface temperature anomaly from (solid black) CESM SMYLE and (dashed) observations, (column 2) likelihood of marine heatwaves as % of model ensemble members at increasing lead-time, and (column 3) likelihood of ocean acidification extremes (Ω_a) as % of model ensemble members at increasing lead-time; masked by areas significantly skillful in the historical period at given forecast lead-time the relative to 1,000 random forecasts at the 95% confidence interval.

Methods

0.4 CESM SMYLE

CESM SMYLE was developed in the CESM2 framework, and includes explicit rendering of marine biogeochemistry with the Marine Biogeochemistry Library (MARBL), configured with three explicit phytoplankton functional groups (diatoms, diazotrophs, and picophytoplankton), one implicit group (calcifiers), a single zooplankton type, multi-nutrient co-limitation (N, P, Si, Fe), and prognostic marine carbonate chemistry across 62 vertical model levels and nominal 1^o horizontal resolution [52–55]. CESM SMYLE was initialized from the SMYLE Forced Ocean-Sea Ice (FOSI) reconstruction, an ocean-sea ice only simulation forced with the Japanese 55-year Reanalysis (JRA-55; [56]) momentum, heat, and freshwater fluxes from 1958 to 2019 and atmospheric CO_2 concentrations. CESM SMYLE was initialized four times per year (February 1, May 1, August 1, November 1) from 1970-2019 with an integration time of 2 years. A slight perturbation of surface air temperature is included at each initialization to generate 20 ensemble members. More detail on the Community Earth System Model (CESM) Seasonal to Multiyear Large Ensemble (SMYLE) hindcast can be found in Yeager et al., 2022 [40] and Mogen et al., 2023 [37]. Output utilized in this study is saved at monthly temporal resolution. Alongside the hindcast initializations of CESM SMYLE (1970-2019), we also analyze a CESM SMYLE forecast initialized in November 2023 from the SMYLE FOSI that was extended using near real-time updates to the JRA55-do ocean/sea-ice forcing dataset [56]. See Figure S7 for an example of two initializations of CESM SMYLE (November, 2006; November, 2009) in the hindcast period.

0.5 Observational Products

MHW and OAX events were identified in the observational record based on OceanSODA-ETHZ, which interpolates surface ocean partial pressure of CO_2 (pCO_2; from the Surface Ocean CO_2 Atlas) [SOCAT; 57] and Alkalinity (from the Global Ocean Data Analysis Project) [GLODAP2; 58] observations using machine learning techniques [59] at nominal 1^o horizontal resolution and monthly temporal resolution. Global Alkalinity and pCO_2 estimates are then used to solve the full carbonate system using PyCO2SYS to generate estimates for all carbonate tracers [60]. Sea surface temperature is from Operational Sea Surface Temperature and Sea Ice Analysis [61, 62]. OceanSODA-ETHZ includes historical data from 1982-2022, is well validated, and has been used in prior studies on marine carbonate chemistry [63] and extremes [5].

0.6 Defining Extremes

We calculate statistical extremes using the definition widely adopted in the literature [9, 10, 22]. Figure S8 displays the relative magnitude of statistical extremes in comparison to seasonal, interannual, and multidecadal variability. While seasonal variability is prominent in the extratropical oceans, the magnitude of extremes can be as large, if not larger than the other sources of variability in the tropics and northeast Pacific (Figure S8). We remove the long-term, anthropogenic trend and the seasonal climatology for SST, Ω_a, and $[H^+]$ at each grid cell in observations and CESM SMYLE as in Jacox et al, 2022 [8]. We choose to remove long-term anthropogenic warming and acidification trends in our assessment of extreme events in order to account for shifting baselines in marine ecosystems as suggested by Amaya et al. 2023 [64]. In observations, MHWs are defined by first removing seasonal climatologies and long-term warming trends (1st order polynomial). Then a rolling three-monthly threshold is created centered on the month of interest and the 90^{th} percentile threshold is calculated. In CESM SMYLE, a similar procedure was followed by first removing model climatology and long-term trends (along the dimension of year of initialization) from each ensemble member. Then a rolling three-lead-time (three monthly) threshold was calculated, centered on the lead-time (month) of interest. Values above this threshold were again considered extreme. This methodology was repeated for $[H^+]$ (removing a 2nd order polynomial trend, extreme above the 90^{th} percentile) and Ω_a (removing a 2nd order polynomial trend, extreme below the 10^{th} percentile). We process the November, 2023 SMYLE Initialization in the same manner as for November-initialized hindcast. As noted above, Ω_a is most detrimental to marine organisms when below saturation ($\Omega_a < 1$), but we choose to rely on a statistical definition of extremes following prior work [23, 65]. The usefulness of statistical definitions of extremes may have a limit in comparison to a threshold based on an absolute value (e.g., assuming organisms have limited adaptability outside of statistical thresholds, rather than an absolute stress threshold), but they prove useful when assessing skill across multiple forms of extremes across the global ocean as noted by Gruber et al. 2021 [66]. See Figure S7 for example of the appearance of OAX (Ω_a) in CESM SMYLE and SMYLE FOSI in the hindcast period.

0.7 Impacts of El Niño-Southern Oscillation

Principal component analysis (PCA) was completed for variables of interest (SST, Ω_a, and $[H^+]$) from SMYLE FOSI over the hindcast period (1982-2019) in the tropical pacific (30°S to 30°N, and 140°E to 280°E) by computing eigenvalues/eigenvectors of spatially weighted anomaly covariance matrices. The standardized first principal components of SST, Ω_a, and $[H^+]$ were compared to a 5 month running mean of the Niño3.4 index (SST anomalies from 5°S-5°N and 170°W-120°W). The first principal components were then regressed onto SMYLE FOSI anomalies to illustrate the spatial patterns associated with the leading principical components (EOFs) for each tracer. Anomaly correlation coefficients were calculated for the first principal component of each variable of interest and the running Niño index, with significance estimated at the 95% confidence interval.

In an effort to disentangle the drivers of $[H^+]$ and Ω_a variability, the linear impact of temperature on $[H^+]$ was determined using the pyCO2SYS software [60] by varying temperature and holding all other inputs constant at their climatological mean values. Temperature effects are removed by calculating the $[H^+]$ variability driven by the thermal component ($[H^+]_t$) throughout the model historical record and subtracting that from $[H^+]$, leaving the nonthermal component ($[H^+]_{nt}$). Principal component analysis was then repeated for nonthermal values to determine the dominant modes of variability with the temperature effects removed.

To determine the impact of ENSO state at initialization on model forecast skill, we separate forecasts by those initialized during El Niño (Nino3.4 SSTa greater than 0.5^{o}C)and La Ninã (Nino3.4 SSTa less than -0.5^{o}C) and those initialized during neutral ENSO state (Nino3.4 SSTa between -0.5^{o}C and 0.5^{o}C). We then assess skill for these separate forecasts and take the difference in forecast skill at each lead-time to determine the impact of ENSO-state at initialization.

0.8 Drivers of Ω_a forecast skill

We analyze drivers of OAX (Ω_a), using the model definition of Ω_a:

$$\Omega_a \approx \frac{[CO_3^{2-}]}{[CO_3]_{saturation,aragonite}} \tag{1}$$

where $[CO_3]^{2-}$ and $[CO_3]^{2-}_{saturation,aragonite}$ are estimated at each model timestep. Change during extremes are driven by $[CO_3]^{2-}$, as $[CO_3]^{2-}_{saturation,aragonite}$ is largely a function of pressure. The expected changes in $[CO_3]^{2-}$ during extreme event are decomposed into contributions from temperature, salinity, dissolved inorganic carbon (DIC), and alkalinity using relationships derived with pyCO2sys [60]. We take the difference between periods of extreme events and all times, indicating which are the most important terms in driving changes in Ω_a. We decompose the DIC response to extreme events using model output tendency terms, including: total DIC tendency, air-sea CO_2 flux, and biological flux. Circulation tendency is calculated as the residual:

$$DIC_{circulation,tendency} = DIC_{tendency} - Air\ Sea\ Flux_{tendency} - Biological_{tendency} \tag{2}$$

As with $[CO_3]^{2-}$ we take the difference between tendency terms during extreme events and all times.

0.9 Skill Analysis

We combine all annual initializations for analysis of skill (relative to OceanSODA-ETHZ) and predictability (relative to SMYLE FOSI), as previous literature has found little impacts of initialization month on global ocean biogeochemical forecast skill (e.g. Mogen et al. 2023) [37]. Combining initializations further increased the number of forecasts being evaluated, increasing the statistical robustness of results. To assess forecast skill, we follow established methodologies for evaluating relatively infrequent climatic extremes: the SEDI skill score, Forecast Accuracy, and Brier Skill Score. First, we classify each grid cell at each time into a 2X2 contingency table: true positives (extreme event is forecast and does appear in observations), false positive (extreme event is forecast but does not appear), false negative (extreme event is not forecast but does appear), and true negatives (extreme event is not forecast and does not appear). Using this contingency table, we then calculate SEDI and forecast accuracy. We also calculated the Brier Skill Score based on the average of the binary forecasts from all ensemble members at a given time.

We follow Jacox et al., 2022[8] in using SEDI as our primary skill metric. As noted in their work, it does not trend towards a meaningless limit as rarity increases, it is base-rate independent (not influenced by changes in event frequency), and it is equitable (random forecasts give an expected value of zero, or no skill). SEDI

scores of greater than zero indicates skill better than random chance, while skill of less than zero indicates worse than random chance of an event being forecast correctly [8, 67, 68]:

$$SEDI = \frac{logF - logH - log(1-F) + log(1-H)}{logF + logH + log(1-F) + log(1-H)} \tag{3}$$

where H is the hit rate (rate of true positives to total observed events) and F is the false alarm rate (rate of false positives to total observed nonevents).

Significance of SEDI forecast skill is quantified using a Monte Carlo simulation with bootstrapping. For a given grid cell, we randomly sample (with replacement) each SMYLE forecast to generate random forecasts; skill is then calculated for random forecasts. This process is repeated 1,000 times to generate a distribution of random forecasts. We then calculate the 95% confidence interval for scores of the random forecast at each grid cell. Skill scores are considered significant if the forecast exceeds the 97.5th percentile of random forecast skill distribution.

We use the contingency table to calculate Forecast Accuracy, which is simply the fraction of correctly forecast events [8]:

$$FA = \frac{true\ positives + true\ negatives}{N} \tag{4}$$

where N is the total number of forecasts being evaluated. For events that occur 10% of the time (as in this study for all metrics), the forecast accuracy for a random forecast is calculated as 0.82.

We also calculate the Brier Skill Score (BSS). First, the Brier Score (BrS) estimates the mean square error of the probabilistic forecast:

$$BrS = \frac{1}{N}\sum_{i=1}^{N}(f_i - o_i)^2 \tag{5}$$

where N is the number of forecasts evaluated, f_i is the forecast probability from all ensemble members, o_i is the observed probability (zero or one). The Brier Score is then normalized relative to a reference forecast where events have a 10% chance of occurring:

$$BSS = 1 - \frac{BrS}{BrS_{ref}} \tag{6}$$

The resulting BSS ranges from one (perfect) to negative infinity, with zero indicating skill no better than random chance.

References

[1] Doney, Scott C. et al. “Ocean Acidification: The Other CO $_2$ Problem”. en. *Annual Review of Marine Science* **1** (Jan. 2009), 169–192. ISSN: 1941-1405, 1941-0611. DOI: 10.1146/annurev.marine.010908.163834. URL: https://www.annualreviews.org/doi/10.1146/annurev.marine.010908.163834 (visited on 10/27/2022).

[2] Bopp, L. et al. “Multiple stressors of ocean ecosystems in the 21st century: projections with CMIP5 models”. en. *Biogeosciences* **10** (Oct. 2013), 6225–6245. ISSN: 1726-4189. DOI: 10.5194/bg-10-6225-2013. URL: https://bg.copernicus.org/articles/10/6225/2013/ (visited on 10/27/2022).

[3] Kwiatkowski, Lester and Orr, James C. “Diverging seasonal extremes for ocean acidification during the twenty-first century”. en. *Nature Climate Change* **8** (Feb. 2018), 141–145. ISSN: 1758-678X, 1758-6798. DOI: 10.1038/s41558-017-0054-0. URL: http://www.nature.com/articles/s41558-017-0054-0 (visited on 10/27/2022).

[4] Heinze, Christoph et al. *Reviews and syntheses: Abrupt ocean biogeochemical change under human-made climatic forcing – warming, acidification, and deoxygenation*. preprint. Biogeochemistry: Open Ocean, Oct. 2023. DOI: 10.5194/bg-2023-182. URL: https://bg.copernicus.org/preprints/bg-2023-182/ (visited on 10/24/2023).

[5] Mogen, Samuel C. et al. “Ocean Biogeochemical Signatures of the North Pacific Blob”. en. *Geophysical Research Letters* **49** (May 2022). ISSN: 0094-8276, 1944-8007. DOI: 10.1029/2021GL096938. URL: https://onlinelibrary.wiley.com/doi/10.1029/2021GL096938 (visited on 10/27/2022).

[6] Frölicher, Thomas L. and Laufkötter, Charlotte. “Emerging risks from marine heat waves”. en. *Nature Communications* **9** (Dec. 2018), 650. ISSN: 2041-1723. DOI: 10.1038/s41467-018-03163-6. URL: http://www.nature.com/articles/s41467-018-03163-6 (visited on 10/27/2022).

[7] Kohlman, Catherine et al. *The 2019 Marine Heatwave at Ocean Station Papa: A multi-disciplinary assessment of ocean conditions and impacts on marine ecosystems*. en. preprint. Preprints, July 2023. DOI: 10.22541/essoar.168881965.57429860/v1. URL: https://essopenarchive.org/users/633226/articles/651717-the-2019-marine-heatwave-at-ocean-station-papa-a-multi-disciplinary-assessment-of-ocean-conditions-and-impacts-on-marine-ecosystems?commit=dbc5570bcbdd6ac200d0db5a01468eafb5452760 (visited on 11/06/2023).

[8] Jacox, Michael G. et al. "Global seasonal forecasts of marine heatwaves". en. *Nature* **604** (Apr. 2022), 486–490. ISSN: 0028-0836, 1476-4687. DOI: 10.1038/s41586-022-04573-9. URL: https://www.nature.com/articles/s41586-022-04573-9 (visited on 12/14/2022).

[9] Hobday, Alistair J. et al. "A hierarchical approach to defining marine heatwaves". en. *Progress in Oceanography* **141** (Feb. 2016), 227–238. ISSN: 00796611. DOI: 10.1016/j.pocean.2015.12.014. URL: https://linkinghub.elsevier.com/retrieve/pii/S0079661116000057 (visited on 10/27/2022).

[10] Holbrook, Neil J. et al. "A global assessment of marine heatwaves and their drivers". en. *Nature Communications* **10** (Dec. 2019), 2624. ISSN: 2041-1723. DOI: 10.1038/s41467-019-10206-z. URL: http://www.nature.com/articles/s41467-019-10206-z (visited on 10/27/2022).

[11] Di Lorenzo, Emanuele and Mantua, Nathan. "Multi-year persistence of the 2014/15 North Pacific marine heatwave". en. *Nature Climate Change* **6** (Nov. 2016), 1042–1047. ISSN: 1758-678X, 1758-6798. DOI: 10.1038/nclimate3082. URL: http://www.nature.com/articles/nclimate3082 (visited on 10/27/2022).

[12] Amaya, Dillon J. et al. "Physical drivers of the summer 2019 North Pacific marine heatwave". en. *Nature Communications* **11** (Dec. 2020), 1903. ISSN: 2041-1723. DOI: 10.1038/s41467-020-15820-w. URL: http://www.nature.com/articles/s41467-020-15820-w (visited on 10/27/2022).

[13] Scannell, Hillary et al. *Spatiotemporal Evolution of Marine Heatwaves Globally*. en. preprint. Preprints, July 2023. DOI: 10.22541/essoar.169008275.57053412/v1. URL: https://essopenarchive.org/users/641800/articles/655898-spatiotemporal-evolution-of-marine-heatwaves-globally?commit=6f3826de74003a9b7435bbdb48e8377fb8487db9 (visited on 10/02/2023).

[14] Guo, Xiuwen et al. "Threat by marine heatwaves to adaptive large marine ecosystems in an eddy-resolving model". en. *Nature Climate Change* **12** (Feb. 2022), 179–186. ISSN: 1758-678X, 1758-6798. DOI: 10.1038/s41558-021-01266-5. URL: https://www.nature.com/articles/s41558-021-01266-5 (visited on 10/27/2022).

[15] Wyatt, Abigale M., Resplandy, Laure, and Marchetti, Adrian. "Ecosystem impacts of marine heat waves in the northeast Pacific". en. *Biogeosciences* **19** (Dec. 2022), 5689–5705. ISSN: 1726-4189. DOI: 10.5194/bg-19-5689-2022. URL: https://bg.copernicus.org/articles/19/5689/2022/ (visited on 11/28/2023).

[16] Rühmkorff, Sarah et al. "Marine heatwaves and upwelling shape stress responses in a keystone predator". en. *Proceedings of the Royal Society B: Biological Sciences* **290** (Jan. 2023), 20222262. ISSN: 0962-8452, 1471-2954. DOI: 10.1098/rspb.2022.2262. URL: https://royalsocietypublishing.org/doi/10.1098/rspb.2022.2262 (visited on 01/23/2023).

[17] Welch, Heather et al. "Impacts of marine heatwaves on top predator distributions are variable but predictable". en. *Nature Communications* **14** (Sept. 2023), 5188. ISSN: 2041-1723. DOI: 10.1038/s41467-023-40849-y. URL: https://www.nature.com/articles/s41467-023-40849-y (visited on 01/09/2024).

[18] Smale, Dan A. et al. "Marine heatwaves threaten global biodiversity and the provision of ecosystem services". en. *Nature Climate Change* **9** (Apr. 2019), 306–312. ISSN: 1758-678X, 1758-6798. DOI: 10.1038/s41558-019-0412-1. URL: https://www.nature.com/articles/s41558-019-0412-1 (visited on 01/09/2024).

[19] Fragkopoulou, Eliza et al. "Marine biodiversity exposed to prolonged and intense subsurface heatwaves". en. *Nature Climate Change* (Sept. 2023). ISSN: 1758-678X, 1758-6798. DOI: 10.1038/s41558-023-01790-6. URL: https://www.nature.com/articles/s41558-023-01790-6 (visited on 10/02/2023).

[20] Hauri, C. et al. "Spatiotemporal variability and long-term trends of ocean acidification in the California Current System". en. *Biogeosciences* **10** (Jan. 2013), 193–216. ISSN: 1726-4189. DOI: 10.5194/bg-10-193-2013. URL: https://bg.copernicus.org/articles/10/193/2013/ (visited on 10/27/2022).

[21] Hauri, Claudine, Friedrich, Tobias, and Timmermann, Axel. “Abrupt onset and prolongation of aragonite undersaturation events in the Southern Ocean”. en. *Nature Climate Change* **6** (Feb. 2016), 172–176. ISSN: 1758-678X, 1758-6798. DOI: 10.1038/nclimate2844. URL: https://www.nature.com/articles/nclimate2844 (visited on 11/14/2023).

[22] Burger, Friedrich A., John, Jasmin G., and Frölicher, Thomas L. “Increase in ocean acidity variability and extremes under increasing atmospheric CO2”. en. *Biogeosciences* **17** (Sept. 2020), 4633–4662. ISSN: 1726-4189. DOI: 10.5194/bg-17-4633-2020. URL: https://bg.copernicus.org/articles/17/4633/2020/ (visited on 10/27/2022).

[23] Burger, Friedrich A. and Frölicher, Thomas L. “Drivers of Surface Ocean Acidity Extremes in an Earth System Model”. en. *Global Biogeochemical Cycles* **37** (Sept. 2023), e2023GB007785. ISSN: 0886-6236, 1944-9224. DOI: 10.1029/2023GB007785. URL: https://agupubs.onlinelibrary.wiley.com/doi/10.1029/2023GB007785 (visited on 10/02/2023).

[24] Desmet, Flora et al. “Tracking the Space-Time Evolution of Ocean Acidification Extremes in the California Current System and Northeast Pacific”. en. *Journal of Geophysical Research: Oceans* **127** (May 2022). ISSN: 2169-9275, 2169-9291. DOI: 10.1029/2021JC018159. URL: https://onlinelibrary.wiley.com/doi/10.1029/2021JC018159 (visited on 10/27/2022).

[25] Wong, Joel, Münnich, Matthias, and Gruber, Nicolas. *Column-Compound Extremes in the Global Ocean*. en. Oct. 2023. DOI: 10.22541/essoar.169755245.55770848/v1. URL: https://essopenarchive.org/users/671079/articles/670763-column-compound-extremes-in-the-global-ocean?commit=f04802600f7de02fe402e3535a909f6313744812 (visited on 04/09/2024).

[26] Desmet, Flora et al. “Tracking the Space-Time Evolution of Ocean Acidification Extremes in the California Current System and Northeast Pacific”. en. *Journal of Geophysical Research: Oceans* **127** (May 2022). ISSN: 2169-9275, 2169-9291. DOI: 10.1029/2021JC018159. URL: https://onlinelibrary.wiley.com/doi/10.1029/2021JC018159 (visited on 02/27/2023).

[27] Mucci, A. “The solubility of calcite and aragonite in seawater at various salinities, temperatures, and one atmosphere total pressure”. en. *American Journal of Science* **283** (Sept. 1983), 780–799. ISSN: 0002-9599. DOI: 10.2475/ajs.283.7.780. URL: https://ajsonline.org/article/60282 (visited on 04/15/2024).

[28] Ries, J. B., Cohen, A. L., and McCorkle, D. C. “Marine calcifiers exhibit mixed responses to CO2-induced ocean acidification”. en. *Geology* **37** (Dec. 2009), 1131–1134. ISSN: 0091-7613, 1943-2682. DOI: 10.1130/G30210A.1. URL: https://pubs.geoscienceworld.org/geology/article/37/12/1131-1134/103987 (visited on 03/18/2024).

[29] Bednaršek, Nina et al. “Systematic Review and Meta-Analysis Toward Synthesis of Thresholds of Ocean Acidification Impacts on Calcifying Pteropods and Interactions With Warming”. en. *Frontiers in Marine Science* **6** (May 2019), 227. ISSN: 2296-7745. DOI: 10.3389/fmars.2019.00227. URL: https://www.frontiersin.org/article/10.3389/fmars.2019.00227/full (visited on 04/09/2024).

[30] Negrete-García, Gabriela et al. “Sudden emergence of a shallow aragonite saturation horizon in the Southern Ocean”. en. *Nature Climate Change* **9** (Apr. 2019), 313–317. ISSN: 1758-678X, 1758-6798. DOI: 10.1038/s41558-019-0418-8. URL: https://www.nature.com/articles/s41558-019-0418-8 (visited on 03/18/2024).

[31] Bednaršek, Nina et al. “Pteropods on the edge: Cumulative effects of ocean acidification, warming, and deoxygenation”. en. *Progress in Oceanography* **145** (June 2016), 1–24. ISSN: 00796611. DOI: 10.1016/j.pocean.2016.04.002. URL: https://linkinghub.elsevier.com/retrieve/pii/S0079661115300112 (visited on 10/27/2022).

[32] Bednaršek, Nina et al. “El Niño-Related Thermal Stress Coupled With Upwelling-Related Ocean Acidification Negatively Impacts Cellular to Population-Level Responses in Pteropods Along the California Current System With Implications for Increased Bioenergetic Costs”. en. *Frontiers in Marine Science* **5** (Dec. 2018), 486. ISSN: 2296-7745. DOI: 10.3389/fmars.2018.00486. URL: https://www.frontiersin.org/article/10.3389/fmars.2018.00486/full (visited on 10/27/2022).

[33] Bednaršek, N. et al. “Exposure history determines pteropod vulnerability to ocean acidification along the US West Coast”. en. *Scientific Reports* **7** (July 2017), 4526. ISSN: 2045-2322. DOI: 10.1038/s41598-017-03934-z. URL: https://www.nature.com/articles/s41598-017-03934-z (visited on 10/26/2023).

[34] Bednaršek, Nina et al. “Integrated Assessment of Ocean Acidification Risks to Pteropods in the Northern High Latitudes: Regional Comparison of Exposure, Sensitivity and Adaptive Capacity”. en. *Frontiers in Marine Science* **8** (Sept. 2021), 671497. ISSN: 2296-7745. DOI: 10.3389/fmars.2021.671497. URL: https://www.frontiersin.org/articles/10.3389/fmars.2021.671497/full (visited on 10/24/2023).

[35] Manno, Clara, Peck, Victoria L., and Tarling, Geraint A. “Pteropod eggs released at high pCO2 lack resilience to ocean acidification”. en. *Scientific Reports* **6** (May 2016), 25752. ISSN: 2045-2322. DOI: 10.1038/srep25752. URL: https://www.nature.com/articles/srep25752 (visited on 11/14/2023).

[36] Stock, Charles A. et al. “Seasonal sea surface temperature anomaly prediction for coastal ecosystems”. en. *Progress in Oceanography* **137** (Sept. 2015), 219–236. ISSN: 00796611. DOI: 10.1016/j.pocean.2015.06.007. URL: https://linkinghub.elsevier.com/retrieve/pii/S0079661115001408 (visited on 10/27/2022).

[37] Mogen, Samuel C. et al. “Skillful Multi-Month Predictions of Ecosystem Stressors in the Surface and Subsurface Ocean”. en. *Earth's Future* **11** (Nov. 2023), e2023EF003605. ISSN: 2328-4277, 2328-4277. DOI: 10.1029/2023EF003605. URL: https://agupubs.onlinelibrary.wiley.com/doi/10.1029/2023EF003605 (visited on 11/06/2023).

[38] Brady, Riley X. et al. “Skillful multiyear predictions of ocean acidification in the California Current System”. en. *Nature Communications* **11** (Dec. 2020), 2166. ISSN: 2041-1723. DOI: 10.1038/s41467-020-15722-x. URL: http://www.nature.com/articles/s41467-020-15722-x (visited on 10/27/2022).

[39] McAdam, Ronan, Masina, Simona, and Gualdi, Silvio. “Seasonal forecasting of subsurface marine heatwaves”. en. *Communications Earth & Environment* **4** (June 2023), 225. ISSN: 2662-4435. DOI: 10.1038/s43247-023-00892-5. URL: https://www.nature.com/articles/s43247-023-00892-5 (visited on 12/06/2023).

[40] Yeager, Stephen G. et al. “The Seasonal-to-Multiyear Large Ensemble (SMYLE) prediction system using the Community Earth System Model version 2”. en. *Geoscientific Model Development* **15** (Aug. 2022), 6451–6493. ISSN: 1991-9603. DOI: 10.5194/gmd-15-6451-2022. URL: https://gmd.copernicus.org/articles/15/6451/2022/ (visited on 10/27/2022).

[41] Jacox, Michael G. et al. “Seasonal-to-interannual prediction of North American coastal marine ecosystems: Forecast methods, mechanisms of predictability, and priority developments”. en. *Progress in Oceanography* **183** (Apr. 2020), 102307. ISSN: 00796611. DOI: 10.1016/j.pocean.2020.102307. URL: https://linkinghub.elsevier.com/retrieve/pii/S007966112030046X (visited on 10/27/2022).

[42] Capotondi, Antonietta et al. “Predictability of US West Coast Ocean Temperatures is not solely due to ENSO”. en. *Scientific Reports* **9** (Dec. 2019), 10993. ISSN: 2045-2322. DOI: 10.1038/s41598-019-47400-4. URL: http://www.nature.com/articles/s41598-019-47400-4 (visited on 12/14/2022).

[43] Capotondi, A. et al. “An Optimal Precursor of Northeast Pacific Marine Heatwaves and Central Pacific El Niño Events”. en. *Geophysical Research Letters* **49** (Mar. 2022), e2021GL097350. ISSN: 0094-8276, 1944-8007. DOI: 10.1029/2021GL097350. URL: https://agupubs.onlinelibrary.wiley.com/doi/10.1029/2021GL097350 (visited on 04/30/2024).

[44] Ren, Xianglin et al. “The Pacific Decadal Oscillation modulated marine heatwaves in the Northeast Pacific during past decades”. en. *Communications Earth & Environment* **4** (June 2023), 218. ISSN: 2662-4435. DOI: 10.1038/s43247-023-00863-w. URL: https://www.nature.com/articles/s43247-023-00863-w (visited on 04/30/2024).

[45] Sarmiento, Jorge L. and Gruber, Nicolas. *Ocean Biogeochemical Dynamics*. Princeton University Press, July 2013. ISBN: 978-1-4008-4907-9 978-0-691-01707-5. DOI: 10.2307/j.ctt3fgxqx. URL: http://www.jstor.org/stable/10.2307/j.ctt3fgxqx (visited on 01/16/2024).

[46] Lovenduski, Nicole S. et al. “The Potential Impact of Nuclear Conflict on Ocean Acidification”. en. *Geophysical Research Letters* **47** (Feb. 2020), e2019GL086246. ISSN: 0094-8276, 1944-8007. DOI: 10.1029/2019GL086246. URL: https://agupubs.onlinelibrary.wiley.com/doi/10.1029/2019GL086246 (visited on 01/16/2024).

[47] Reynolds, Richard W. et al. “Daily High-Resolution-Blended Analyses for Sea Surface Temperature”. en. *Journal of Climate* **20** (Nov. 2007), 5473–5496. ISSN: 1520-0442, 0894-8755. DOI: 10.1175/2007JCLI1824.1. URL: http://journals.ametsoc.org/doi/10.1175/2007JCLI1824.1 (visited on 04/22/2024).

[48] Lilly, Laura E. et al. “Biogeochemical Anomalies at Two Southern California Current System Moorings During the 2014–2016 Warm Anomaly-El Niño Sequence”. en. *Journal of Geophysical Research: Oceans* **124** (Oct. 2019), 6886–6903. ISSN: 2169-9275, 2169-9291. DOI: 10.1029/2019JC015255. URL: https://onlinelibrary.wiley.com/doi/10.1029/2019JC015255 (visited on 10/27/2022).

[49] Mills, Katherine E. et al. “Ocean ecosystems and marine resources”. *Fifth National Climate Assessment*. Ed. by A.R. Crimmins et al. Section: 10 Type: Book Section. Washington, DC, USA: U.S. Global Change Research Program, 2023. DOI: 10.7930/NCA5.2023.CH10.

[50] Siedlecki, Samantha A. et al. “Experiments with Seasonal Forecasts of ocean conditions for the Northern region of the California Current upwelling system”. en. *Scientific Reports* **6** (June 2016), 27203. ISSN: 2045-2322. DOI: 10.1038/srep27203. URL: https://www.nature.com/articles/srep27203 (visited on 02/03/2023).

[51] Brodie, Stephanie et al. “Ecological forecasts for marine resource management during climate extremes”. en. *Nature Communications* **14** (Dec. 2023), 7701. ISSN: 2041-1723. DOI: 10.1038/s41467-023-43188-0. URL: https://www.nature.com/articles/s41467-023-43188-0 (visited on 01/09/2024).

[52] Moore, J. Keith et al. “An intermediate complexity marine ecosystem model for the global domain”. en. *Deep Sea Research Part II: Topical Studies in Oceanography* **49** (Jan. 2001), 403–462. ISSN: 09670645. DOI: 10.1016/S0967-0645(01)00108-4. URL: https://linkinghub.elsevier.com/retrieve/pii/S0967064501001084 (visited on 10/27/2022).

[53] Moore, J. Keith, Doney, Scott C., and Lindsay, Keith. “Upper ocean ecosystem dynamics and iron cycling in a global three-dimensional model: GLOBAL ECOSYSTEM-BIOGEOCHEMICAL MODEL”. en. *Global Biogeochemical Cycles* **18** (Dec. 2004), n/a–n/a. ISSN: 08866236. DOI: 10.1029/2004GB002220. URL: http://doi.wiley.com/10.1029/2004GB002220 (visited on 10/27/2022).

[54] Moore, J. Keith et al. “Marine Ecosystem Dynamics and Biogeochemical Cycling in the Community Earth System Model [CESM1(BGC)]: Comparison of the 1990s with the 2090s under the RCP4.5 and RCP8.5 Scenarios”. en. *Journal of Climate* **26** (Dec. 2013), 9291–9312. ISSN: 0894-8755, 1520-0442. DOI: 10.1175/JCLI-D-12-00566.1. URL: https://journals.ametsoc.org/doi/10.1175/JCLI-D-12-00566.1 (visited on 10/27/2022).

[55] Long, Matthew C. et al. “Simulations With the Marine Biogeochemistry Library (MARBL)”. en. *Journal of Advances in Modeling Earth Systems* **13** (Dec. 2021). ISSN: 1942-2466, 1942-2466. DOI: 10.1029/2021MS002647. URL: https://onlinelibrary.wiley.com/doi/10.1029/2021MS002647 (visited on 01/30/2023).

[56] Tsujino, Hiroyuki et al. “JRA-55 based surface dataset for driving ocean–sea-ice models (JRA55-do)”. en. *Ocean Modelling* **130** (Oct. 2018), 79–139. ISSN: 14635003. DOI: 10.1016/j.ocemod.2018.07.002. URL: https://linkinghub.elsevier.com/retrieve/pii/S146350031830235X (visited on 04/22/2024).

[57] Bakker, Dorothee C. E. et al. “A multi-decade record of high-quality <i>f</i>CO₂ data in version 3 of the Surface Ocean CO₂ Atlas (SOCAT)”. en. *Earth System Science Data* **8** (Sept. 2016), 383–413. ISSN: 1866-3516. DOI: 10.5194/essd-8-383-2016. URL: https://essd.copernicus.org/articles/8/383/2016/ (visited on 10/27/2022).

[58] Olsen, Are et al. “GLODAPv2.2019 – an update of GLODAPv2”. en. *Earth System Science Data* **11** (Sept. 2019), 1437–1461. ISSN: 1866-3516. DOI: 10.5194/essd-11-1437-2019. URL: https://essd.copernicus.org/articles/11/1437/2019/ (visited on 11/16/2023).

[59] Gregor, Luke and Gruber, Nicolas. “OceanSODA-ETHZ: a global gridded data set of the surface ocean carbonate system for seasonal to decadal studies of ocean acidification”. en. *Earth System Science Data* **13** (Mar. 2021), 777–808. ISSN: 1866-3516. DOI: 10.5194/essd-13-777-2021. URL: https://essd.copernicus.org/articles/13/777/2021/ (visited on 10/27/2022).

[60] Humphreys, Matthew P. et al. *PyCO2SYS v1.7: marine carbonate system calculations in Python*. en. preprint. Oceanography, June 2021. DOI: 10.5194/gmd-2021-159. URL: https://gmd.copernicus.org/preprints/gmd-2021-159/gmd-2021-159.pdf (visited on 10/27/2022).

[61] Good, S.A. et al. *ESA Sea Surface Temperature Climate Change Initiative (SST_cci): Level 4 Analysis Climate Data Record, version 2.0*. en. 2019. DOI: 10.5285/ACED40D7CB964F23A0FD3E85772F2D48. URL: https://catalogue.ceda.ac.uk/uuid/aced40d7cb964f23a0fd3e85772f2d48 (visited on 01/08/2024).

[62] Good, Simon et al. “The Current Configuration of the OSTIA System for Operational Production of Foundation Sea Surface Temperature and Ice Concentration Analyses”. en. *Remote Sensing* **12** (Feb. 2020), 720. ISSN: 2072-4292. DOI: 10.3390/rs12040720. URL: https://www.mdpi.com/2072-4292/12/4/720 (visited on 01/08/2024).

[63] Ma, Danling, Gregor, Luke, and Gruber, Nicolas. “Four Decades of Trends and Drivers of Global Surface Ocean Acidification”. en. *Global Biogeochemical Cycles* **37** (July 2023), e2023GB007765. ISSN: 0886-6236, 1944-9224. DOI: 10.1029/2023GB007765. URL: https://agupubs.onlinelibrary.wiley.com/doi/10.1029/2023GB007765 (visited on 12/11/2023).

[64] Amaya, Dillon J. et al. “Marine heatwaves need clear definitions so coastal communities can adapt”. en. *Nature* **616** (Apr. 2023), 29–32. ISSN: 0028-0836, 1476-4687. DOI: 10.1038/d41586-023-00924-2. URL: https://www.nature.com/articles/d41586-023-00924-2 (visited on 01/09/2024).

[65] Hauri, Claudine et al. “More Than Marine Heatwaves: A New Regime of Heat, Acidity, and Low Oxygen Compound Extreme Events in the Gulf of Alaska”. en. *AGU Advances* **5** (Feb. 2024), e2023AV001039. ISSN: 2576-604X, 2576-604X. DOI: 10.1029/2023AV001039. URL: https://agupubs.onlinelibrary.wiley.com/doi/10.1029/2023AV001039 (visited on 04/09/2024).

[66] Gruber, Nicolas et al. “Biogeochemical extremes and compound events in the ocean”. en. *Nature* **600** (Dec. 2021), 395–407. ISSN: 0028-0836, 1476-4687. DOI: 10.1038/s41586-021-03981-7. URL: https://www.nature.com/articles/s41586-021-03981-7 (visited on 10/27/2022).

[67] Marshall, A. G. et al. “Intra-seasonal drivers of extreme heat over Australia in observations and POAMA-2”. en. *Climate Dynamics* **43** (Oct. 2014), 1915–1937. ISSN: 0930-7575, 1432-0894. DOI: 10.1007/s00382-013-2016-1. URL: http://link.springer.com/10.1007/s00382-013-2016-1 (visited on 10/25/2023).

[68] Ferro, Christopher A. T. and Stephenson, David B. “Extremal Dependence Indices: Improved Verification Measures for Deterministic Forecasts of Rare Binary Events”. en. *Weather and Forecasting* **26** (Oct. 2011), 699–713. ISSN: 0882-8156, 1520-0434. DOI: 10.1175/WAF-D-10-05030.1. URL: https://journals.ametsoc.org/doi/10.1175/WAF-D-10-05030.1 (visited on 10/25/2023).

[69] Yeager, Stephen. *Seasonal-to-Multiyear Large Ensemble (SMYLE) Experiment [Dataset]*. 2022. DOI: 10.26024/PWMA-RE41. URL: https://www.earthsystemgrid.org/dataset/id/e475ba3c-2c0d-4f38-929c-0db96d5fe937.html (visited on 07/18/2023).

* Corresponding author: samuel.mogen@colorado.edu

Acknowledgments

SCM and NSL were supported by the National Science Foundation (OCE 1752724) and the National Oceanic and Atmospheric Administration (NA20OAR4310405). MPB was supported by the National Oceanic and Atmospheric Administration (NA20OAR4310405). SY and NR acknowledge support from the Regional and Global Model Analysis (RGMA) component of the Earth and Environmental System Modeling Program of the U.S. Department of Energy’s Office of Biological & Environmental Research (BER) under Award Number DE-SC0022070. WK and SY acknowledge the support of NOAA Climate Program Office’s CVP program under grant #NA20OAR4310408. AC was supported by the NOAA Climate Program Office’s MAPP program, DOE Award #DE-SC0023228, and NASA Physical Oceanography grant #80NSSC21K0556. This work also was supported by the National Center for Atmospheric Research, which is a major facility sponsored by the National Science Foundation (NSF) under Cooperative Agreement No. 1852977. We thank the National Center for Atmospheric Research Earth System Working Group for their development of invaluable software tools used in processing CESM SMYLE: https://github.com/CESM-ESPWG/ESP-Lab. We are grateful for helpful feedback from Dillon Amaya.

Author Contributions

S.C.M and N.S.L. designed the study. S.C.M. performed the analysis. All authors contributed to interpretation of the results. S.C.M. and N.S.L. wrote the manuscript with input from all authors.

Data availability

The CESM Seasonal to Multiyear Large Ensemble and SMYLE FOSI are available at: https://doi.org/10.26024/pwmare41 [69]. OceanSODA-ETHZ can be accessed at https://doi.org/10.25921/m5wx-ja34[59].

Code availability

Code used in processing and analyzing CESM SMYLE output can be found at DOI 10.5281/zenodo.12103992.

Competing interests

The authors declare no competing interests.

1 Supporting Information

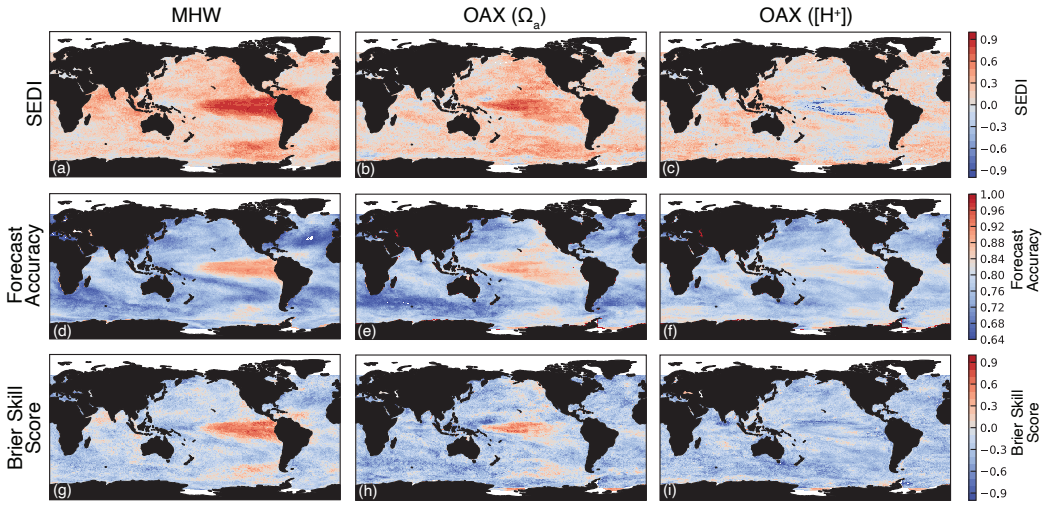

Figure S1: Forecast skill calculated by three different metrics at lead-time 3.5 months. SEDI (as in Figure 1) (row 1), Forecast Accuracy (row 2), and Brier Skill Score (BSS) (row 3) for marine heatwaves (column 1), ocean acidification extremes (Ω_a), and ocean acidification extremes ($[H^+]$)

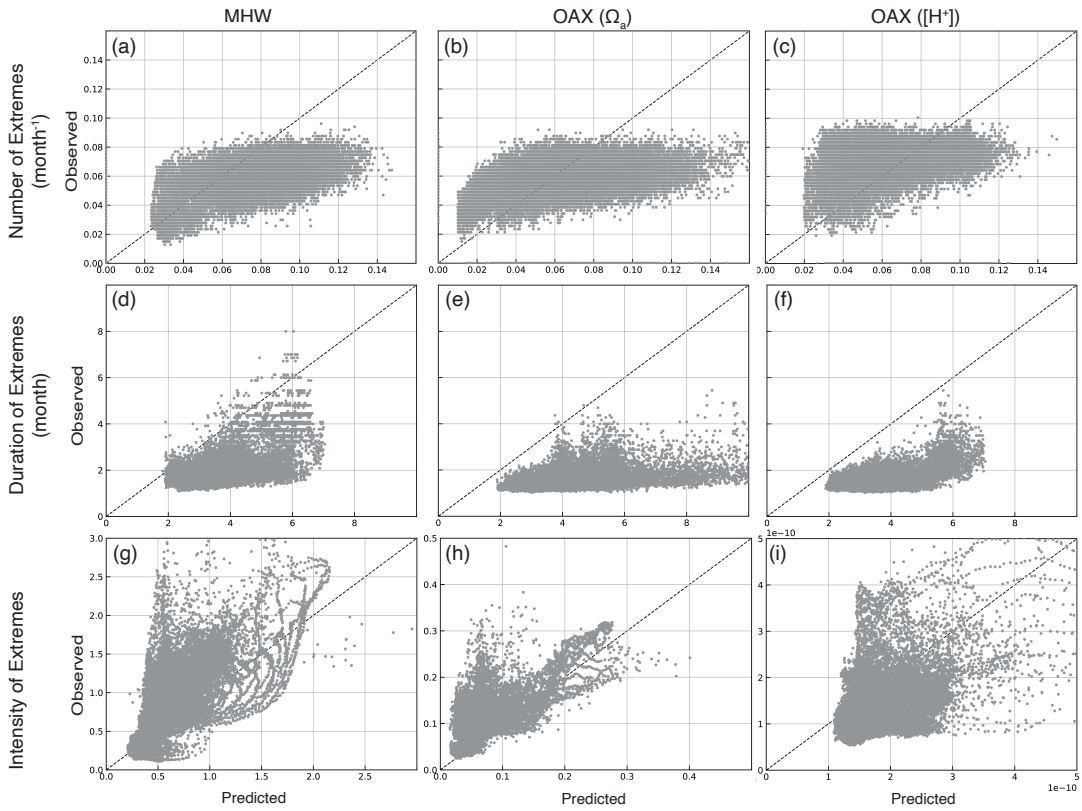

Figure S2: Number per month (row 1), duration (row 2), and intensity (row 3) of the average extreme event in observations and CESM SMYLE for marine heatwaves (column 1), ocean acidification extremes (Ω_a) (column 2), and ocean acidification extremes ($[H^+]$) (column 3) at each location.

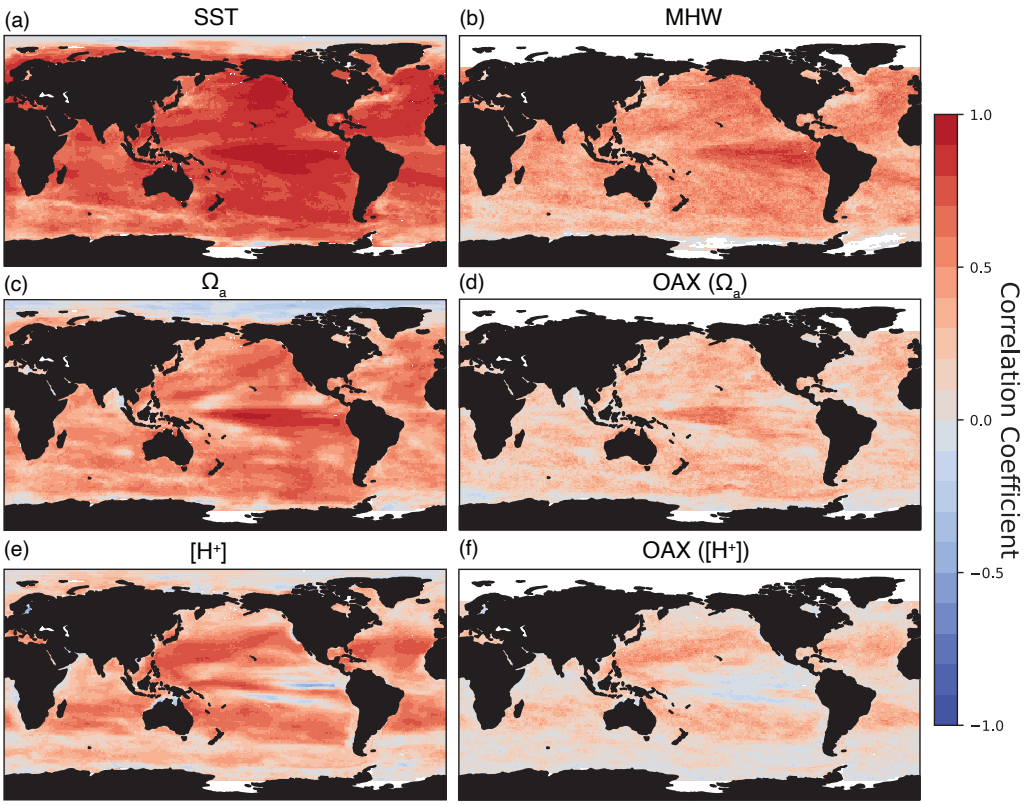

Figure S3: Correlation coefficient between historical (column 1) variability of (a) sea surface temperature, (c) Ω_a, (e) $[H^+]$ and (column 2) extremes (b) marine heatwaves, (d) ocean acidification extremes (Ω_a),(f) ocean acidification extremes ($[H^+]$) in SMYLE FOSI and observations (OceanSODA-ETHZ). Higher correlation coefficients indicate more similar historical variability or extreme events.

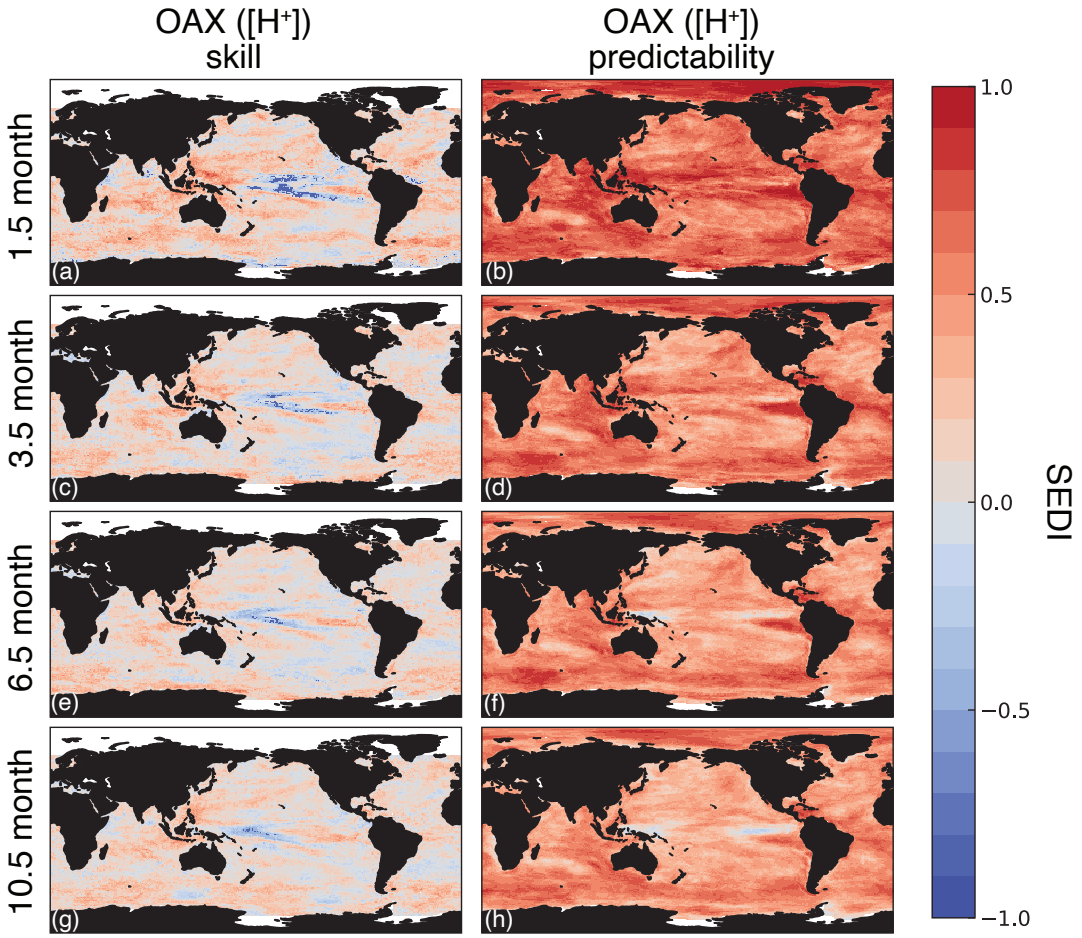

Figure S4: Comparison of (column 1) model skill (CESM SMYLE relative to observations) and (column 2) model predictability (CESM SMYLE relative to SMYLE FOSI) for 20 ensemble members from CESM SMYLE at 1.5 (a-b), 3.5 (c-d), 6.5 (e-f), and 10.5 month lead-time (g-h). Skill scores range from -1 to 1, with SEDI score close to -1 being unskillful, SEDI score of 0 being no better than random forecasts, and SEDI score of 1 being perfect skill.

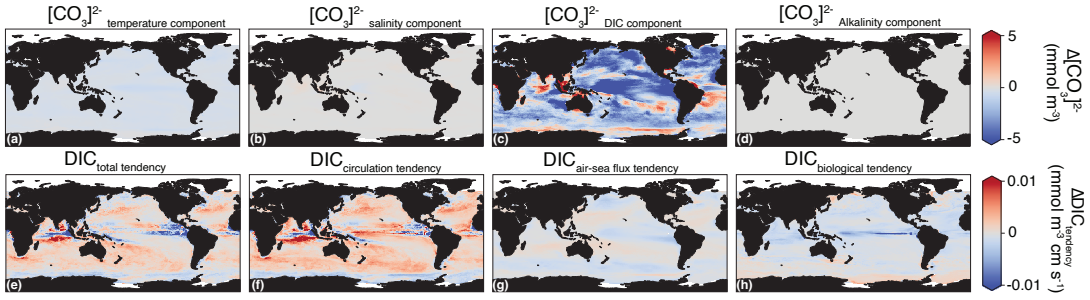

Figure S5: Decomposition of Ω_a to determine drivers of extreme events. (row 1) Decomposition of $[CO_3]^{2-}$ into drivers of changes during extremes relative to all times, including effects of (a) temperature, (b) salinity, (c) DIC, (d) Alkalinity. (row 2) Changes to tendency terms of DIC during extremes relative to all times, including: (e) total DIC tendency, (f) circulation tendency, (g) air-sea CO_2 flux tendency, and (h) biological tendency.

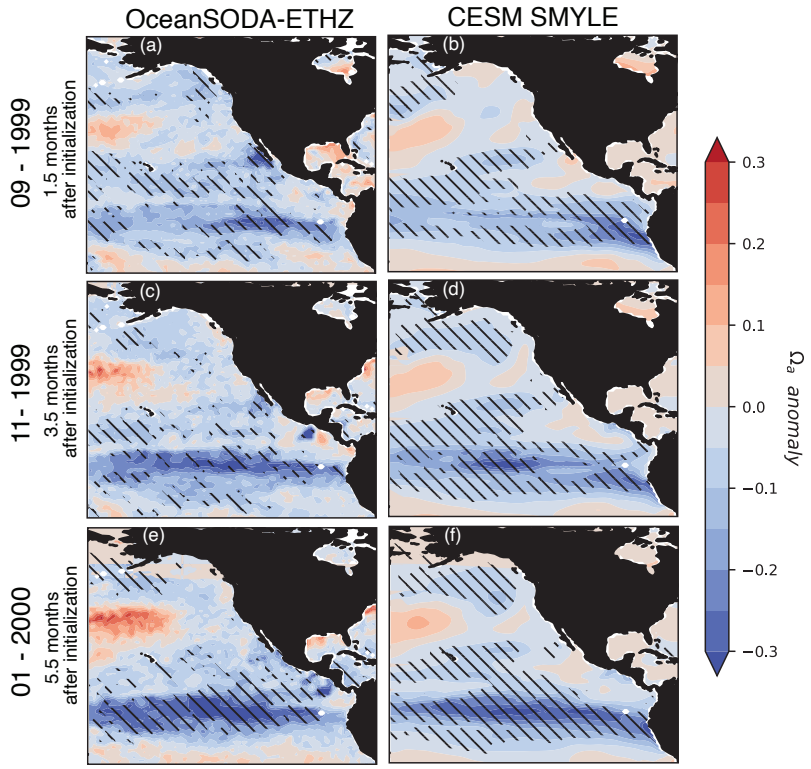

Figure S6: Forecasts of Ω_a initialized during the August 1999 La Niña event. Anomalies (color) and extremes (hatching) in (column 1) from an interpolated observational product (OceanSODA-ETHZ), and (column 2) CESM SMYLE forecasts (a,b) 1.5, (c,d) 3.5, and (e,f) 5.5 months after initialization. Extreme events are defined in observations (below the 10^{th} percentile) and in CESM SMYLE (below the 10^{th} percentile in a minimum of 50% of ensemble members).

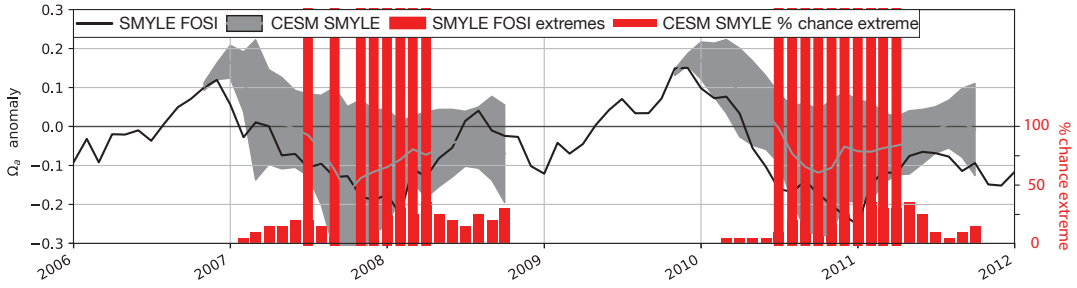

Figure S7: Example timeseries of Ω_a anomalies in the central tropical Pacific (0.5^{o}N, 138.5^{o}W) for (black) SMYLE FOSI and (grey) two November CESM SMYLE initializations (2006a and 2009; with ensemble spread represented) from 2006-2012. Occurrence of extreme events are indicated for (red lines) SMYLE FOSI and (bar plot) CESM SMYLE (as a percentage of ensemble members).

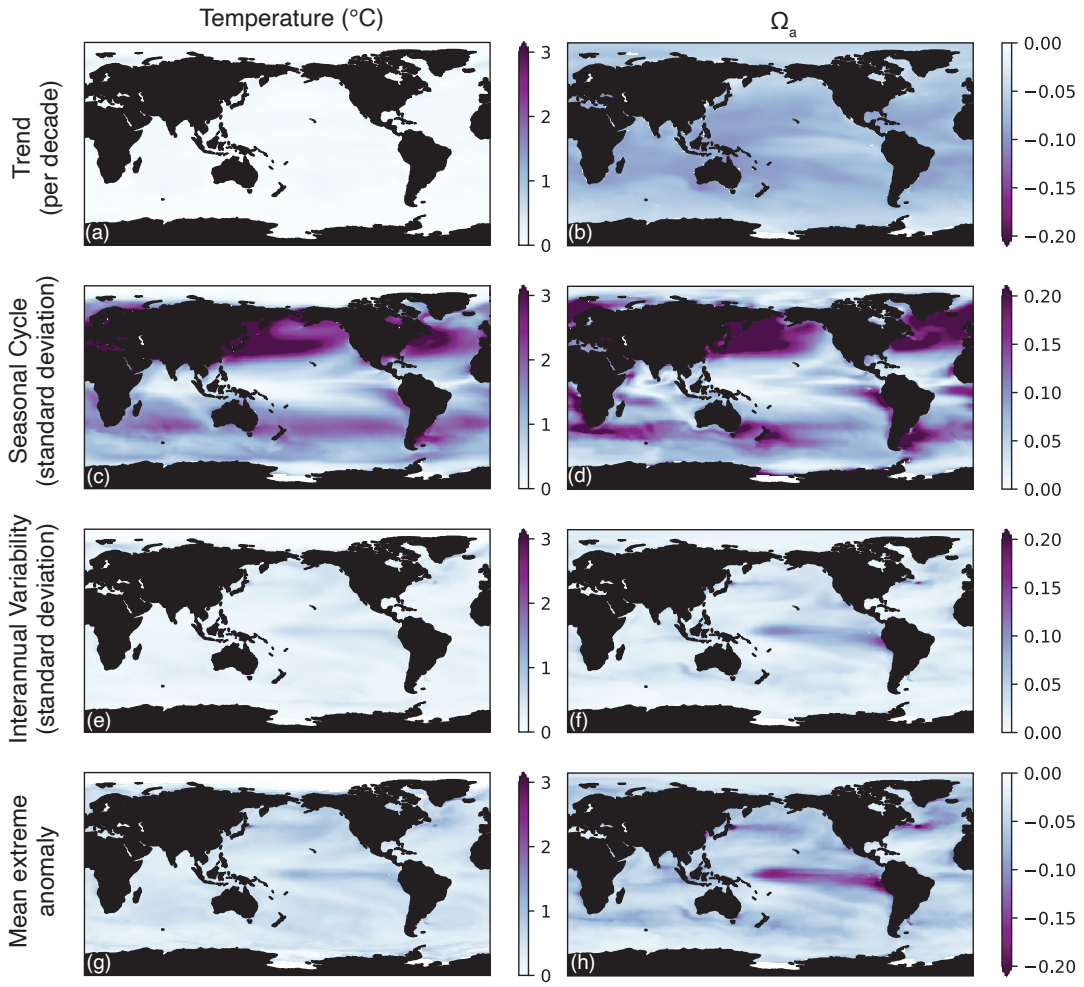

Figure S8: Relative magnitude of anomalies associated with (row 1) trend (per decade), (row 2) seasonal climatology, (row 3) interannual variability, and (row 4) mean strength of anomaly to generate extreme event for temperature and Ω_a.